

September 06, 2011

Spin texture on the warped Dirac-cone surface states in topological insulators

Susmita Basak
Northeastern University

Hsin Lin
Northeastern University

L. A. Wray
Princeton University

S. Y. Xu
Princeton University

L. Fu
Harvard University

See next page for additional authors

Recommended Citation

Basak, Susmita; Lin, Hsin; Wray, L. A.; Xu, S. Y.; Fu, L.; Hasan, M. Z.; and Bansil, A., "Spin texture on the warped Dirac-cone surface states in topological insulators" (2011). *Physics Faculty Publications*. Paper 430. <http://hdl.handle.net/2047/d20004207>

Author(s)

Susmita Basak, Hsin Lin, L. A. Wray, S. Y. Xu, L. Fu, M. Z. Hasan, and A. Bansil

Spin texture on the warped Dirac-cone surface states in topological insulators

Susmita Basak,¹ Hsin Lin,¹ L. A. Wray,^{2,3} S.-Y. Xu,^{2,3} L. Fu,⁴ M. Z. Hasan,^{2,3} and A. Bansil¹

¹*Department of Physics, Northeastern University, Boston, Massachusetts 02115, USA*

²*Joseph Henry Laboratories of Physics, Princeton University, Princeton, New Jersey 08544, USA*

³*Princeton Center for Complex Materials, Princeton University, Princeton, New Jersey 08544, USA*

⁴*Department of Physics, Harvard University, Cambridge, Massachusetts 02138, USA*

(Received 24 April 2011; published 6 September 2011)

We have investigated the nature of surface states in the Bi_2Te_3 family of three-dimensional topological insulators using first-principles calculations as well as a model Hamiltonian approach. When the surface Dirac cone is warped due to Dresselhaus spin-orbit coupling in rhombohedral structures, the spin acquires a finite out-of-the-plane component. We provide a simple, minimal model to describe the in-plane spin texture of the warped surface Dirac cone observed in experiments where spins are seen to be *not* aligned perpendicular to the electron momentum. Our $k \cdot p$ model calculation reveals that this in-plane spin texture requires fifth-order Dresselhaus spin-orbit coupling terms.

DOI: [10.1103/PhysRevB.84.121401](https://doi.org/10.1103/PhysRevB.84.121401)

PACS number(s): 73.20.-r, 73.43.Cd

Topological insulators (TIs)¹⁻⁹ realize a unique state of quantum matter that is distinguished by topological invariants of bulk band structure rather than spontaneously broken symmetries. Its material realization in two-dimensional (2D) artificial HgTe quantum wells⁷⁻⁹ and three-dimensional (3D) Bi-based compounds¹⁰⁻¹³ has led to a worldwide surge of interest in different topological physics. The surfaces of 3D topological insulators or the interface between two materials with distinct topological invariants host metallic surface and/or interface states. Electrons on the surface of an ideal topological insulator have an energy-momentum relationship in the shape of a Dirac cone. In the presence of such a single-Dirac-cone surface or interface band, a number of exotic quantum phenomena have been predicted.¹⁴⁻¹⁷ Recent spin-resolved photoemission measurements reveal that the spins of the electrons on the surface Dirac cone are locked with their momenta, giving rise to helical Dirac fermions without spin degeneracy.^{3,4,10,18-20} This one-to-one locking of the electron spin to the momentum comes from a combination of strong spin-orbit interaction and the breaking of the inversion symmetry at the surface. Such a spin texture on the surface Dirac cone leads to antilocalization properties and plays a central role in inducing exotic quantum phenomena.

Recent angle-resolved photoemission (ARPES) experiments have observed the surface Dirac cone in a number of topological insulators.^{4,11,18} In particular, Bi_2Te_3 exhibits a Dirac cone with significant hexagonal warping,^{4,11,18,21} i.e., the shape of Fermi surface (FS) or constant energy contours evolves from an ideal circle to a hexagon to being snowflake-like with increasing energy. The hexagonal distortion of the cone does not change the associated Berry phase quantifying its topological invariant, consistent with its topological order.^{4,11} Fu²¹ proposed that Dresselhaus spin-orbit coupling can lead to hexagonal warping of the Dirac cone in rhombohedral structures. The spins then acquire finite out-of-the-plane components through the orbital channel to conserve the net value of the Berry's phase. The resulting finite value of the out-of-the-plane component opens up unique possibilities for unusual phenomena such as the enhancement of interference patterns around crystal defects and exotic magnetic orders at the surface.

In this Rapid Communication, we investigate the nature of surface states in the Bi_2Te_3 family of three-dimensional topological insulators using first-principles calculations as well as a model Hamiltonian approach. We reproduce a warped surface Dirac cone with finite out-of-the-plane spin component, and provide an alternate generalized model to describe the in-plane spin texture where spins are *not* aligned perpendicular to the electron momentum as observed in experiments.²² This different $k \cdot p$ model requires fifth-order Dresselhaus spin-orbit coupling terms. This is a generic property of surface states in strong spin-orbit coupling materials, and not limited to the topological insulators.

Bi_2Te_3 is a semiconductor with a rhombohedral crystal structure (space group $R\bar{3}m$). The unit cell contains five atoms with quintuple layers ordered in the Te(1)-Bi-Te(2)-Bi-Te(1) sequence. Due to weak bonds between the two Te(1) atoms in the adjacent quintuple layers, the (111) surface with Te(1) termination can be easily obtained and is the surface usually studied in experiments and used here. We computed surface states by using a symmetric 30-layer slab in a hexagonal unit cell. Band calculations were performed with the full-potential linear augmented plane-wave (LAPW) method with the WIEN2K package.²³ The generalized gradient approximation (GGA) was used to describe the exchange-correlation potential.²⁴ Spin-orbit coupling was included as a second variational step using scalar-relativistic eigenfunctions as the basis. After self-consistent charges and potentials were obtained, we added an extra potential on one side of the slab during band computations to remove the degeneracy between the two surfaces of a symmetric slab. It should be noted that our analysis which is based on dispersions does not address matrix element effects, which are important for describing spectral intensities in scanning tunneling microscopy (STM),²⁵ ARPES,²⁶ inelastic light scattering,^{27,28} and other²⁹ highly resolved spectroscopies.

We show the computed surface bands (red/dark gray lines) and the projected bulk band structure (green/light gray area) in Fig. 1(a) along the high-symmetry directions in the surface Brillouin zone (BZ). Note that the lower Dirac portion of the cone has a particularly distorted shape [inset in Fig. 1(a)]. The insulating phase of the bulk is predicted with a 45-meV

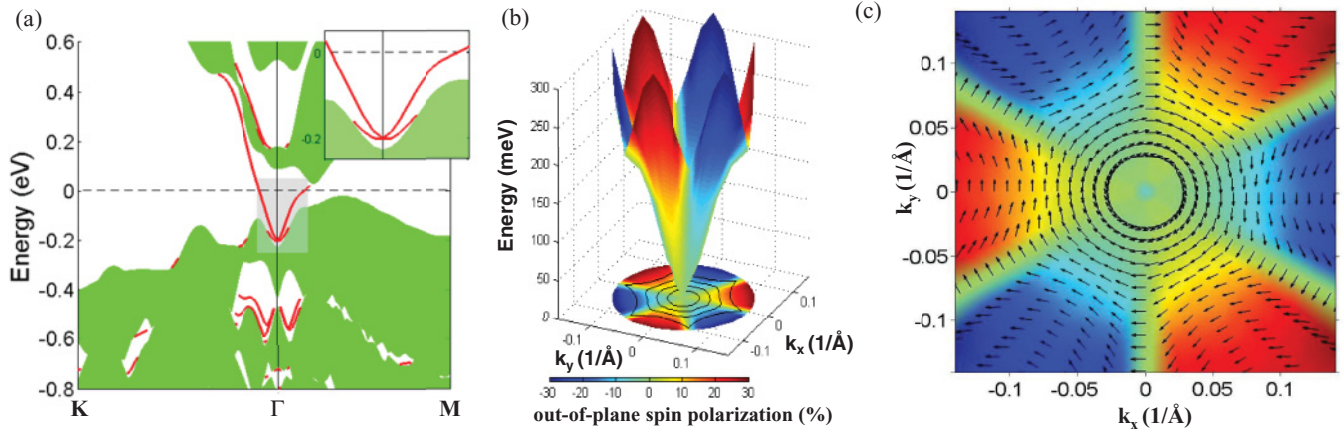


FIG. 1. (Color online) (a) Electronic structure of Bi_2Te_3 . Surface states are shown by red (dark gray) lines and projected bulk bands by the green/light gray area. The inset is a blowup of the rectangular light gray area. (b) Energy dependence of Bi_2Te_3 surface Dirac cone showing hexagonal warping. Magnitude of out-of-the-plane spin component is indicated by the color bar. (c) In-plane direction of spin on the surface Dirac cone.

indirect gap, while the experimental value is 165 meV.⁴ This underestimation of band gap is typical of the GGA exchange functional. Between the Γ and M points, an odd number (one in this case) of surface bands is seen to cross the Fermi level (E_F). This is the hallmark of the topological insulator. Topological nontriviality can also be established by evaluating the time-reversal invariant Z_2 parameter using a wave-function parity analysis.² The value of Z_2 is thus found to be -1 due to a single-band inversion at the Γ point.

Topological surface states form a Dirac-cone-like band dispersion in the energy-momentum space as shown in Fig. 1(b). The shapes of the energy contours for the upper Dirac cone [projected onto the $E = 0$ plane in Fig. 1(b)] are circles for the low-energy region, but become hexagonal at ~ 150 meV above the Dirac point. The hexagonal warping becomes more pronounced at higher energies above ~ 200 meV, where a snowflakelike shape emerges. These surface states have been observed in ARPES experiments^{4,11,18,21} and the hexagonal warping effect has been described in a $k \cdot p$ model.²¹ Recent Fourier-transform scanning tunneling microscopy (FT-STM) experiments have shown the nontrivial interference patterns resulting from the nesting of hexagonally warped energy contours.³⁰ When the Dirac cone is warped, it must carry a finite out-of-the-plane spin component. The out-of-the-plane spin component has threefold symmetry with up- and down-spin alternation around a circle, whereas the band dispersion displays sixfold symmetry. Since the mirror plane is along the Γ - M direction (chosen to be the y direction), the out-of-the-plane spin component has to be zero along this direction, as shown in Fig. 1(b). The in-plane spin texture in Fig. 1(c) demonstrates the unique phenomenon of nonorthogonality between spin and momentum. The helical nature of the spin is preserved at low energies near the Dirac point where the spins remain perpendicular to k . When E is increased, a significant departure from this ideal helical behavior is seen, even though the spin and momentum remain orthogonal to each other along the high-symmetry directions Γ - M and Γ - K . Similar features were also observed in recent photoemission experiments on Bi_2Se_3 ,²² where it was noted that the existing $k \cdot p$ theory

could not explain the in-plane nonorthogonality between the electron spin and momentum. To gain further insight into the origin of this nontrivial behavior of the spins, we have also investigated the surface states of Bi_2Te_3 using a $k \cdot p$ model with higher-order corrections discussed below.

In our formalism, the effective Hamiltonian for the surface bands is expanded up to fifth order in \vec{k} as follows:

$$H(k) = E_0(k) + v_k(k_x\sigma_y - k_y\sigma_x) + \frac{\lambda_k}{2}(k_+^3 + k_-^3)\sigma_z + i\zeta(k_+^5\sigma_+ - k_-^5\sigma_-), \quad (1)$$

where $E_0(k) = k^2/2m_1^* + k^4/2m_2^*$, $k_{\pm} = k_x \pm ik_y$, $\sigma_{\pm} = \sigma_x \pm i\sigma_y$, and the σ_i are the Pauli matrices. The form (1) of $H(k)$ is suitable for describing the [111] surface band structure near the Γ point in the surface BZ of Bi_2Te_3 family of TIs, and it is invariant under time-reversal and C_{3v} symmetries. $E_0(k)$ generates particle-hole asymmetry and the term $H_0(k) = v_k(k_x\sigma_y - k_y\sigma_x)$ describes an isotropic 2D helical Dirac fermion. The Dirac velocity $v_k = v(1 + \alpha k^2 + \beta k^4)$, where v is the Fermi velocity, contains a fourth-order correction term. More importantly, the k^3 term, $H_w = \frac{\lambda_k}{2}(k_+^3 + k_-^3)\sigma_z$, leads to the hexagonal warping of the Fermi surface. The hexagonal warping parameter also has a second-order correction term $\lambda_k = \lambda(1 + \gamma k^2)$. The last term in Eq. (1) describes a fifth-order spin-orbit coupling at the surface of rhombohedral crystal systems, and to the best of our knowledge, it has not been proposed before.^{31,32} The purpose of introducing this term is to explain the nonorthogonality between the in-plane electron spin and momentum, which cannot be reproduced by the k^3 term. Here we assume that the pseudospin σ_i is proportional to the electron's spin \mathbf{s} . We determined the parameters in the model Hamiltonian of Eq. (1) by fitting the spin directions given by the model to the in-plane spin texture obtained via first-principles computations. Specifically, the variation process first involved minimizing the angle between the model and first-principles spin directions. This was followed by a fit to the first-principles bands to obtain the

TABLE I. Parameters used in the Hamiltonian of Eq. (1).

Parameters	Bi ₂ Te ₃
m_1^* (in eV ⁻¹ Å ⁻²)	35.21
m_2^* (in eV ⁻² Å ⁻⁴)	38.46
v (in eV Å)	-0.0005
α (in eV Å ²)	14.82
λ (in eV Å ³)	-0.04
β (in eV Å ⁵)	-1.26
γ (in eV Å ⁵)	-0.001
ζ (in eV Å ⁵)	0.35

correct energy scale. The final values of the parameters are listed in Table I.

The in-plane spin polarization obtained from our model calculations agrees with the first-principles result and captures the key nonorthogonality effect between the electron spin and momentum. For a quantitative analysis, in Fig. 2(a) we plot the angle θ between the spin direction obtained from the $k \cdot p$ theory and k_x direction (i.e., the Γ -K direction) as a function of the azimuthal angle ϕ at a binding energy of -30 meV. For

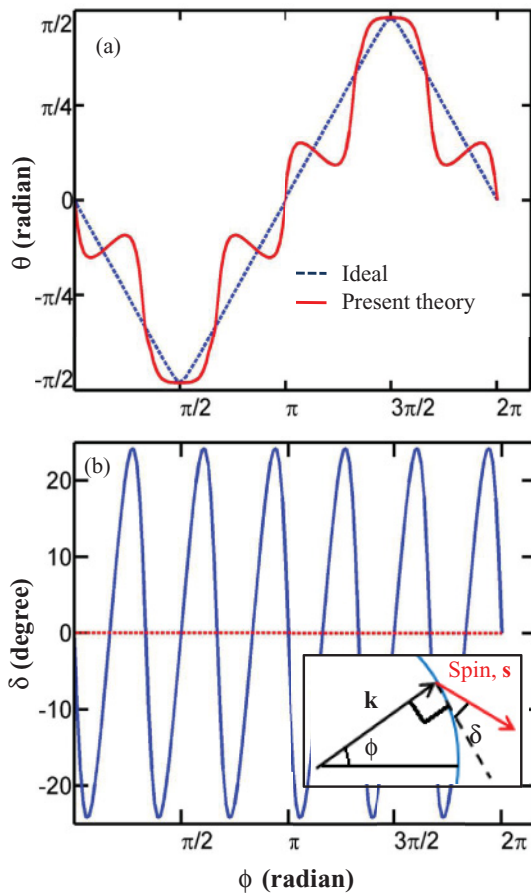


FIG. 2. (Color online) Quantitative analysis of nonorthogonality of electron spin and momentum on the surface Dirac cone of Bi₂Te₃. (a) Angle θ between the spin s and k_x direction obtained from $k \cdot p$ theory is plotted against the azimuthal angle ϕ at a binding energy of -30 meV. The blue dashed curve is the ideal case and the solid red curve gives the results of present theory. (b) Angle of deviation δ (inset) vs ϕ . The inset defines various angles.

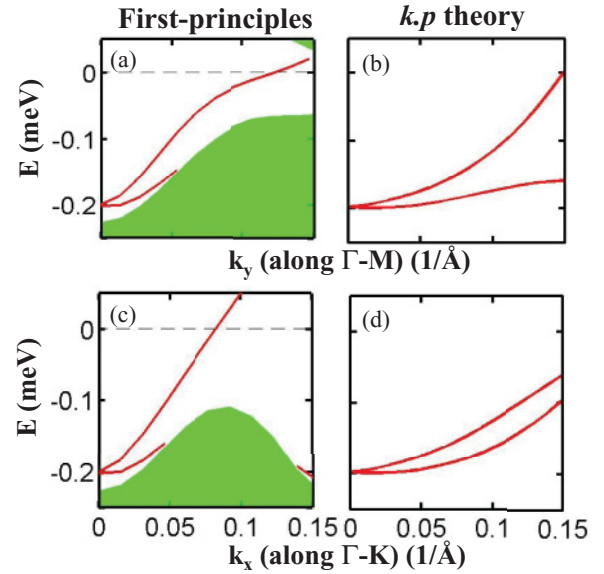


FIG. 3. (Color online) Dispersion of the surface states of Bi₂Te₃. Left-hand panels (a) and (c) are for first-principles calculations. Right-hand panels (b) and (d) are for the $k \cdot p$ model.

ideal helical spins, θ would follow the blue dashed line, but our calculated spins follow the red curve displaying a complicated pattern of spin canting. The calculated angle is equal to the ideal angle only along the high-symmetry directions where the two curves intersect. In Fig. 2(b) we highlight the deviation of the angle between spin and momentum from orthogonality by plotting the angle of deviation δ as a function of the angle ϕ (see the inset for definitions of the angles involved). The deviation δ is seen to oscillate about zero as we move along a constant energy contour in the higher k region where the k^5 term dominates, making the nonorthogonal feature more prominent. Here also we find that δ is exactly equal to 0 along Γ - M and Γ - K directions, indicating that electron spin and momentum remain orthogonal along high-symmetry directions in k space.

Figure 3 shows the surface-state dispersions obtained from the $k \cdot p$ model along the Γ - M [Fig. 3(b)] and Γ - K directions [Fig. 3(d)]. The dispersion is seen to start out linear in momentum k , as expected for a massless Dirac cone, but both the lower and upper branches rapidly deviate from linearity, becoming convex functions of k , similar to the GGA results shown in Figs. 3(a) and 3(c). The STM studies of Bi₂Se₃ and ARPES studies of Bi₂Te₃ and Bi₂Se₃ display a similar surface-state behavior.^{10,33,34} Also, the $k \cdot p$ model with the k^5 term captures the interesting feature of upward dispersion of the lower branch, which is not obtained with the k^3 term alone.

In conclusion, we have shown that the spin of an electron on the surface of a strongly spin-orbit coupled material is in general not orthogonal to the electron momentum due to higher-order Dresselhaus spin-orbit coupling terms in the Hamiltonian. This effect will exist in topological insulators as well as in nontopological metals and insulators. For example, pure bismuth, even though it is topologically trivial, could harbor a unique spin texture. The nonorthogonality of spin and momentum should be observable on the warped surface Dirac cone in the topological insulator Bi₂Te₃, where the spin texture is crucial for a number of exotic quantum phenomena.

We acknowledge important discussions with R. S. Markiewicz. The work at Northeastern and Princeton is supported by the Basic Energy Sciences, US Department of Energy (DE-FG02-07ER46352, DE-FG-02-05ER46200 and AC03-76SF00098), and benefited from the allocation

of supercomputer time at NERSC and Northeastern University's Advanced Scientific Computation Center (ASCC). Support of the A. P. Sloan Foundation (L.A.W. and M.Z.H.) and the Harvard Society of Fellows (L.F.) is acknowledged.

- ¹M. Z. Hasan and C. L. Kane, *Rev. Mod. Phys.* **82**, 3045 (2010).
- ²L. Fu and C. L. Kane, *Phys. Rev. B* **76**, 045302 (2007).
- ³D. Hsieh, D. Qian, L. Wray, Y. Xia, Y. S. Hor, R. J. Cava, and M. Z. Hasan, *Nature (London)* **452**, 970 (2008).
- ⁴D. Hsieh, Y. Xia, D. Qian, L. Wray, J. H. Dil, F. Meier, J. Osterwalder, L. Patthey, J. G. Checkelsky, N. P. Ong, A. V. Fedorov, H. Lin, A. Bansil, D. Grauer, Y. S. Hor, R. J. Cava, and M. Z. Hasan, *Nature (London)* **460**, 1101 (2009).
- ⁵J. E. Moore and L. Balents, *Phys. Rev. B* **75**, 121306(R) (2007).
- ⁶L. Fu, C. L. Kane, and E. J. Mele, *Phys. Rev. Lett.* **98**, 106803 (2007).
- ⁷R. Roy, *Phys. Rev. B* **79**, 195322 (2009).
- ⁸B. A. Bernevig, T. L. Hughes, and S. C. Zhang, *Science* **314**, 1757 (2006).
- ⁹M. König, H. Buhmann, L. W. Molenkamp, T. Hughes, C. X. Liu, X. L. Qi, and S. C. Zhang, *J. Phys. Soc. Jpn.* **77**, 031007 (2008).
- ¹⁰Y. Xia, D. Qian, D. Hsieh, L. Wray, A. Pal, H. Lin, A. Bansil, D. Grauer, Y. S. Hor, R. J. Cava, and M. Z. Hasan, *Nat. Phys.* **5**, 398 (2009).
- ¹¹D. Hsieh, Y. Xia, D. Qian, L. Wray, J. H. Dil, F. Meier, J. Osterwalder, L. Patthey, A. V. Fedorov, H. Lin, A. Bansil, D. Grauer, Y. S. Hor, R. J. Cava, and M. Z. Hasan, *Phys. Rev. Lett.* **103**, 146401 (2009).
- ¹²P. Roushan, J. Seo, C. V. Parker, Y. S. Hor, D. Hsieh, D. Qian, A. Richardella, M. Z. Hasan, R. J. Cava, and Ali Yazdani, *Nature (London)* **460**, 1106 (2009).
- ¹³H. Zhang, C. X. Liu, X. L. Qi, X. Dai, Z. Fang, and S. C. Zhang, *Nat. Phys.* **5**, 438 (2009).
- ¹⁴L. Fu and C. L. Kane, *Phys. Rev. Lett.* **102**, 216403 (2009).
- ¹⁵L. Fu and C. L. Kane, *Phys. Rev. Lett.* **100**, 096407 (2008).
- ¹⁶P. J. Leek, J. M. Fink, A. Blais, R. Bianchetti, M. Göppl, J. M. Gambetta, D. I. Schuster, L. Frunzio, R. J. Schoelkopf, and A. Wallraff, *Science* **318**, 1889 (2007).
- ¹⁷S. A. Wolf, D. D. Awschalom, R. A. Buhrman, J. M. Daughton, S. von Molnár, M. L. Roukes, A. Y. Chtchelkanova, and D. M. Treger, *Science* **294**, 1488 (2001).
- ¹⁸Y. L. Chen, J. H. Chu, J. G. Analytis, Z. K. Liu, K. Igarashi, H.-H. Kuo, X. L. Qi, S.-K. Mo, R. G. Moore, D. H. Lu, M. Hashimoto, T. Sasagawa, S. C. Zhang, I. R. Fisher, Z. Hussain, and Z.-X. Shen, *Science* **329**, 659 (2010).
- ¹⁹A. Nishide, A. A. Taskin, Y. Takeichi, T. Okuda, A. Kakizaki, T. Hirahara, K. Nakatsuji, F. Komori, Y. Ando, and I. Matsuda, *Phys. Rev. B* **81**, 041309(R) (2010).
- ²⁰S. Y. Xu, L. A. Wray, Y. Xia, F. von Rohr, Y. S. Hor, J. H. Dil, F. Meier, B. Slomski, J. Osterwalder, M. Neupane, H. Lin, A. Bansil, A. Fedorov, R. J. Cava, and M. Z. Hasan, e-print [arXiv:1101.3985](https://arxiv.org/abs/1101.3985).
- ²¹L. Fu, *Phys. Rev. Lett.* **103**, 266801 (2009).
- ²²Y. H. Wang, D. Hsieh, D. Pilon, L. Fu, D. R. Gardner, Y. S. Lee, and N. Gedik, e-print [arXiv:1101.5636](https://arxiv.org/abs/1101.5636).
- ²³P. Blaha, K. Schwarz, G. K. H. Madsen, D. Kvasnicka, and J. Luitz, WIEN2K (Tech. Univ., Vienna, 2001).
- ²⁴J. P. Perdew, K. Burke, and M. Ernzerhof, *Phys. Rev. Lett.* **77**, 3865 (1996).
- ²⁵Jouko Nieminen, Hsin Lin, R. S. Markiewicz, and A. Bansil, *Phys. Rev. Lett.* **102**, 037001 (2009); J. Nieminen, I. Suominen, R. S. Markiewicz, H. Lin, and A. Bansil, *Phys. Rev. B* **80**, 134509 (2009).
- ²⁶M. Lindroos and A. Bansil, *Phys. Rev. Lett.* **77**, 2985 (1996); J. C. Campuzano, L. C. Smedskjaer, R. Benedek, G. Jennings, and A. Bansil, *Phys. Rev. B* **43**, 2788 (1991); M. C. Asensio, J. Avila, L. Roca, A. Tejada, G. D. Gu, M. Lindroos, R. S. Markiewicz, and A. Bansil, *ibid.* **67**, 014519 (2003).
- ²⁷R. S. Markiewicz and A. Bansil, *Phys. Rev. Lett.* **96**, 107005 (2006); Y. W. Li, D. Qian, L. Wray, D. Hsieh, Y. Kaga, T. Sasagawa, H. Takagi, R. S. Markiewicz, A. Bansil, H. Eisaki, S. Uchida, and M. Z. Hasan, *Phys. Rev. B* **78**, 073104 (2008).
- ²⁸Y. Tanaka, Y. Sakurai, A. T. Stewart, N. Shiotani, P. E. Mijnders, S. Kaprzyk, and A. Bansil, *Phys. Rev. B* **63**, 045120 (2001); S. Huotari, K. Hämäläinen, S. Manninen, S. Kaprzyk, A. Bansil, W. Caliebe, T. Buslaps, V. Honkimki, and P. Suortti, *ibid.* **62**, 7956 (2000); G. Stutz, F. Wohlert, A. Kaprolat, W. Schlke, Y. Sakurai, Y. Tanaka, M. Ito, H. Kawata, N. Shiotani, S. Kaprzyk, and A. Bansil, *ibid.* **60**, 7099 (1999).
- ²⁹P. E. Mijnders, A. C. Kruseman, A. van Veen, H. Schut, and A. Bansil, *J. Phys. Condens. Matter* **10**, 10383 (1998); L. C. Smedskjaer, A. Bansil, U. Welp, Y. Fang, and K. G. Bailey, *Physica C* **192**, 259 (1992).
- ³⁰Y. Okada, C. Dhital, W. W. Zhou, H. Lin, S. Basak, A. Bansil, Y.-B. Huang, H. Ding, Z. Wang, S. D. Wilson, and V. Madhavan, *Phys. Rev. Lett.* **106**, 206805 (2011).
- ³¹The form of the Hamiltonian explicitly depends on the symmetry of the crystal structure. Bi_2Te_3 has a rhombohedral crystal with C_{3v} symmetry in the presence of a $[111]$ surface. C_{3v} symmetry consists of a threefold rotation C_3 around the trigonal z axis and a mirror operation M under which $x \rightarrow -x$, where x is in the Γ - K direction. The Hamiltonian of Eq. (1) is constructed considering the crystal symmetry, i.e., C_{3v} symmetry and the time-reversal symmetry. The second, third, and fourth terms in the Hamiltonian resemble the Dresselhaus spin-orbit (SO) coupling terms up to the fifth order in \mathbf{k} (see Ref. 32 for details).
- ³²G. Dresselhaus, *Phys. Rev.* **100**, 580 (1955).
- ³³T. Hanaguri, K. Igarashi, M. Kawamura, H. Takagi, and T. Sasagawa, *Phys. Rev. B* **82**, 081305(R) (2010).
- ³⁴Y. L. Chen, J. G. Analytis, J. H. Chu, Z. K. Liu, S.-K. Mo, X. L. Qi, H. J. Zhang, D. H. Lu, X. Dai, Z. Fang, S. C. Zhang, I. R. Fisher, Z. Hussain, and Z.-X. Shen, *Science* **325**, 178 (2009).